Design and Biological Evaluation of 4-Iminohydantoin Sulfamides as New Anti-*Acinetobacter baumannii* Agents

Diana Hodyna[1,*] (ID) **Vasyl Kovalishyn** [1] (ID) , **Ivan Semenyuta** [1] (ID) , **Maryna Kachaeva** [1] , **Yurii Shulha** [1] , **Maksym Bugera** [1] , **Volodymyr Blagodatny** [2] , **Oleh Shablykin** [1] (ID) , **Larysa Metelytsia** [1] (ID)

[1] V.P. Kukhar Institute of Bioorganic Chemistry and Petrochemistry, National Academy of Science of Ukraine, Kyiv, 02094, Ukraine; dianahodyna@gmail.com, (D.H.); vkovalishyn@gmail.com, (V.K.); ivan@bpci.kiev.ua, (I.S.); marinaka4aeva@gmail.com, (M.K.); yuriishulha@ukr.net, (Y.S.); bugera.maksym@gmail.com, (M.B.); shablykin@gmail.com, (O.S.); larisametelitsa@gmail.com, (L.M.)
[2] Shupyk National Healthcare University of Ukraine, 04112, Dorogozhytska Str, 9, Kyiv, Ukraine; vladymyrblago8@gmail.com, (V.B.)
* Correspondence: dianahodyna@gmail.com; (D.H.)

Abstract: With the emergence of multidrug-resistant bacterial strains, there is an urgent need to find antibacterial agents directed at alternative molecular targets. A series of 4-iminohydantoin sulfamides were designed, synthesized, and evaluated as antibacterials. QSAR studies of iminohydantoin's antibacterial activity were made using OCHEM. The predictive ability of the classification models has a balanced accuracy of 83-85%. Validation of the model using a set of external tests showed that the models could be used to predict the activity of newly developed compounds with acceptable accuracy and applicability domain. The models were used to detect a virtual chemical library with the expected activity of compounds against *A. baumannii*. The five most promising compounds were identified, synthesized, and tested. Characterization of these compounds was done by ^{1}H and ^{13}C NMR techniques. The tested iminohydantoin derivatives showed antibacterial activity against studied antibiotic-resistant clinical isolates of *A. baumannii*. Among these derivatives, N-(4-Chlorobenzyl)-N'-[(4Z)-5-(dichloromethylene)-2-oxoimidazolidin-4-ylidene]sulfamide (**8**) was found to be most active with the diameters of bacterial growth inhibition ranging from 18 to 28 mm against all MDR *A. baumannii* strains. Molecular docking results of bioactive compound **8** show the complex form into the active center of *A. baumannii* methionine aminopeptidase with a calculated binding affinity of −9.3 kcal/mol.

Keywords: 4-iminohydantoin sulfamides; QSAR; antibacterial activity; *Acinetobacter baumannii*; docking; methionine aminopeptidase.

1. Introduction

The problem of multiple resistance of the microbial pathogen *Acinetobacter baumannii* is currently widely considered in many literary sources of scientists worldwide [1,2]. It is known that almost a million people worldwide are infected with multidrug-resistant (MDR) strains of *A. baumannii* every year [3]. Antimicrobial therapy for infections caused by multiresistant *A. baumannii* includes such drugs as colistin, sulbactam, and tigecycline, which are used in combination with other antibiotics [4,5]. Published global studies show that the percentage of MDR *A. baumannii* isolates is the highest among all analyzed Gram-negative bacteria [5,6]. *A. baumannii* causes various infections, including ventilator-associated pneumonia, bacteremia, meningitis, urinary tract, wound, and bone infections [7]. The

mortality risk is high and often reaches 40–55% in the intensive care unit [8]. *A. baumannii* is a life-threatening problem due to multidrug resistance and the ability to evade the host's immune response and survive in harsh environmental conditions. Thus, *A. baumannii* is able to survive prolonged drying [9], the formation of protective biofilms, and other conditions [10], which is the basis of antibiotic resistance of *A. baumannii*. *A. baumannii* develops resistance to various antibiotics through its cell-intrinsic and acquired mechanisms. Its ability to induce drug-resistance genes is poorly understood. However, given the ability of the *A. baumannii* genome to exchange genetic material both within species and between species, these bacteria are rapidly evolving towards increased pathogenicity.

In general, the 32 strains of the MDR *A. baumannii* were identified from war-torn patients in the military conflict in Ukraine [11]. Treatment of the wounded is often complicated by infection with *A. baumannii*, which prevents wound healing and causes bacterial meningitis and severe forms of pneumonia [11]. Thus, one of the ways to solve the existing therapeutic problem is to develop new effective pharmacological agents against this infection.

Among a wide range of chemical classes as potential antibiotic agents, heterocyclic compounds with a broad range of biological activity occupy a special place [12,13]. The most common are nitrogen-containing heterocycles or various combinations of the positions of nitrogen, sulfur, and oxygen atoms in five- or six-membered rings. Based on modern statistics, over 85% of all biologically active chemical compounds contain a heterocycle. And it is this fact that reflects the central role of heterocycles in drug development. Using heterocycles is useful in modifying lipophilicity, solubility, polarity, and interactions with biotargets. The use of heterocycles provides a useful tool for modifying solubility, lipophilicity, polarity, and biotarget interactions [14,15].

Iminohydantoin derivatives are well-studied target-oriented compounds with the activity associated with the inhibition of human topoisomerase I [16], BACE1 b-secretase, human serine protease [17], HIV-1 protease [18], and DENV-2 NS2B-NS3 protease [19]. It is known that bacterial aminopeptidases are used as a promising target for the development of new antimicrobial drugs [20,21].

This work presents a series of 4-iminohydantoin sulfamides as potential anti-*A. baumannii* agents using QSAR and docking procedures along with experimental testing.

2. Materials and Methods

2.1. QSAR modeling.

Data. A series of 1073 compounds and their bioactivity against *A. baumannii* were collected from the ChEMBL database [22]. The MIC values of compounds ranged from 0.175 to 2849 µM. The data were divided into high (525 compounds with MIC < 50 µM) and low activity molecules (548 compounds with MIC ≥ 50 µM). An interactive OCHEM platform [23] was used to develop public and freely accessible models for predicting the antimicrobial activity of compounds. Approximately 20% of the compounds were randomly chosen by OCHEM to form independent test sets, while the remaining molecules were used as training sets.

Machine-learning techniques (MLT). Two classical MLT, Associative Neural Networks (ASNNs) and Deep Learning Consensus Architecture (DLCA), were used to build classification QSAR models.

ASNN unites an ensemble of Feed-Forward Backpropagation Neural Networks (FFNNs) with the method of k-Nearest Neighbours (k-NN) [24]. ASNNs use the correlation between ensemble outputs (each molecule is represented in the neural network models space as a vector of model predictions) as a measure of distance between the analyzed cases by the kNNs. This combination corrects the neural network bias and increases its precision. The ensemble comprised 100 neural networks developed using the OCHEM default parameters.

DLCA combines three separate deep-learning neural networks built based on three types of fingerprints by averaging their outputs inside the single neural net and improving the consensus results [25]. In this case, during training, the neural network calculates the best weights for each specific output and for averaging them. As a result, the network provides multitask outputs for each type of fingerprint and a consensus output.

Descriptors. OCHEM supports many software packages for the calculation of diverse molecular descriptors. In the current study, we used E-state indices, AlogPS, and CDK2, which were frequently top-performing descriptors according to our previous studies.

The electrotopological state indices define a molecule's key structural features and combine electronic and topological attributes of the compounds [26].

AlogPS program calculates the estimated lipophilicity (logP) and solubility in water (logS) of chemical compounds [27].

CDK calculates 256 molecular descriptors, such as topological, geometrical, constitutional, electronic, and hybrid descriptors [28].

More details about the descriptors can be found elsewhere [23]. A simple Pearson's pairwise correlation method was used as a filtering method for each descriptor set before they were used as input for the machine-learning methods. The Unsupervised Forward Selection method [29] was applied to select a representative, non-redundant set of descriptors.

Model validation. The initial set of 1073 compounds was split into training (858 compounds) and test (215) sets. Five-fold Cross-Validation (CV) with variable selection was used to estimate the accuracy of the models for the training set [30]. The training data set was split into 5-subsets of approximately equal size. Of the five subsets, only one subset was retained for validation, and the remaining subsets were used for training. After repeating the procedure five times, the statistical coefficients for all 5-test sets were averaged. The predictive performance of the final QSAR model developed with 858 compounds was tested using the test set of 215 compounds.

Estimation of prediction accuracy. The applicability domain (AD) and the prediction accuracy, which are calibrated using CV, are calculated by OCHEM. A probability of incorrect molecular classification based on the standard deviation and average prediction of a model class (PROB-STD), which provided the best classification model's accuracy, was used as a distance-to-model [31]. The model AD corresponded to PROB-STD, covering 90% of molecules within the training set.

Statistical parameters. Statistical parameters, such as sensitivity (SN), specificity (SP), and balanced accuracy (BA), were calculated to assess the predictive power of the binary classifier (see Figure S1 of the Supplementary Materials). The balanced accuracy (BA) denotes a measure of the model's classification quality and is calculated as:

$$BA = (SN + SP)/2$$

The BA is supplemented by a confounding matrix (Figure S1) that shows the number of compounds classified correctly for each class and details of incorrectly classified

compounds, e.g., the number of false positive and the false negative predictions. Detailed information about additional statistical coefficients can be found on the OCHEM website [32].

2.2. Chemistry.

All chemicals and solvents for the synthetic work were acquired from commercial sources and used without further purification. The progress of the reaction was monitored by the TLC method. Melting points were measured by a Fisher-Johns apparatus. ^{1}H and ^{13}C NMR spectra were recorded on Bruker Avance DRX 500 or Varian Mercury 400 spectrometers in DMSO-d_6, taking its residual signals as a standard. Combustion elemental analysis was performed in the V.P. Kukhar Institute of Bioorganic Chemistry and Petrochemistry analytical laboratory. The carbon and hydrogen contents were determined using the Pregl gravimetric method, sulfur – by the Scheininger titrimetric method, nitrogen – using Duma's gasometrical micromethod, chlorine – by the mercurometric method.

The procedure for the synthesis of (Z)-[5-(dichloromethylene)-2-oxoimidazolidin-4-ylidene]sulfamoyl chloride II was described in [33].

Synthesis of (Z)-(5-(dichloromethylene)-2-oxoimidazolidin-4-ylidene)sulfamides 1-3, 6, 8. To a solution of 3.6 mmol of corresponding amine $R^1R^2NH_2$ and 3.6 mmol Et$_3$N in 50 ml of THF at 0-5°C sulfamoyl chloride II (1 g, 3.6 mmol) was added with stirring in portions about 0.1 g. The reaction mixture was stirred at 20-25 °C for 6 h. Then the solvent was evaporated in vacuo. 10 ml of water was added to the residue, and diluted HCl acidfied the mixture. The formed precipitate was filtered off, dried, and recrystallized from ethanol.

Methyl (Z)-3-((N-(5-(dichloromethylene)-2-oxoimidazolidin-4-ylidene)sulfamoyl) amino)propanoate 1. Yield: 1.02 g, 82%; mp: 122-124 °C. ^{1}H NMR (400 MHz, DMSO-d_6) δ 11.10 (br s, 2H), 7.39 (s, 1H), 3.58 (s, 3H), 3.21-3.20 (m, 2H), 2.57-2.55 (m, 2H). ^{13}C NMR (125 MHz, DMSO-d_6) δ 171.4, 152.4, 150.7, 129.9, 106.8, 51.4, 38.8, 33.8. HRMS (ESI) m/z Calcd. for $C_8H_{10}Cl_2N_4O_5S$ (M+H)$^+$ 345.15. Found 346.21. Anal. Calcd., %: C, 27.84; H, 2.92; Cl, 20.54; N, 16.23; S, 9.29. Found, %: C, 27.80; H, 2.90; Cl, 20.65; N, 16.40; S, 9.38.

Ethyl 1-{[(4Z)-5-(Dichloromethylidene)-2-oxoimidazolidin-4-ylidene]sulfamoyl} piperidine4-carboxylate 2 was described in [33].

Methyl (Z)-(N-(5-(dichloromethylene)-2-oxoimidazolidin-4-ylidene)sulfamoyl) glycinate 3. Yield: 1.02 g, 82%; mp: 179-181 °C. ^{1}H NMR (400 MHz, DMSO-d$_6$) δ 11.15 (br s, 2H), 7.78 (s, 1H), 3.84-3.83 (m, 2H), 3.61 (s, 3H). ^{13}C NMR (125 MHz, DMSO-d$_6$) δ 169.7, 162.4, 151.2, 129.8, 107.3, 52.0, 44.0. HRMS (ESI) m/z Calcd. for $C_7H_8Cl_2N_4O_5S$ (M+H)$^+$ 331.5. Found 332.2. Anal. Calcd., %: C, 25.39; H, 2.44; Cl, 21.41; N, 16.92; S, 9.68. Found, %: C, 25.35; H, 2.42; Cl, 21.48; N, 16.98; S, 9.77.

N-[(4Z)-5-(Dichloromethylidene)-2-oxoimidazolidin-4-ylidene]piperidine-1-sulfonamide 6 was described in [33].

N-(4-Chlorobenzyl)-N'-[(4Z)-5-(dichloromethylene)-2-oxoimidazolidin-4-ylidene]sulfamide 8 was described in [33].

2.3. Biology.

The anti-*A. baumannii* activity of the prepared 4-iminohydantoin sulfamides examined by disk diffusion assay in Mueller-Hinton agar [34] against three antibiotic-resistant *A. baumannii* strains. All bacterial strains (*A. baumannii* 1355, *A. baumannii* 1536, *A. baumannii* 725) were obtained from the Museum of Microbial Culture Collection of the Shupyk National

Healthcare University of Ukraine. Petri dishes were incubated with 1×10^5 colony forming units per mL at 37 °C and examined after 24 h. Further dilution of 0.02 ml of the tested compounds was applied to standard paper disks (6 mm) which were placed on the agar plate. The compound content on the disk was 3.0 µM. The tested compounds were dissolved in 0.1% DMSO to which the studied bacterial cultures were not sensitive. The tests were repeated three times. The activity of tested 4-iminohydantoin sulfamides was identified by measuring the zone diameter of the bacterial growth inhibition in millimeters.

2.4. Docking.

SWISS-MODEL homology-modeling server [35] was used to create a homology model. AutoDock Tools (ADT) 1.5.6 was employed to prepare the protein and ligand [36]. All hydrogen atoms have been added to the protein molecule using ADT. All protein atoms were renumbered using the no-bond order method, and the Gasteiger method was used to calculate and add the partial charges and save them in the PDBQT format. The ligand structure and conformation were created using the ChemAxon Marvin Sketch 5.3.735 program [37] and saved in the Mol2 format. The ligand structures were optimized, and the energy was minimized by Avogadro v1.2.0 program [38]. Docking was performed using the AutoDock Vina 1.1.2 program [39]. The docking center was selected as the center of the co-crystallized ligand in the structure PDB ID: 2P98 [40]. A grid of 30*30*30 points with a grid step of 1.0 Å was used. Interaction analysis and visualization were performed by Accelrys DS [41].

3. Results and Discussion

3.1. QSAR prediction.

The initial set (1073 compounds) was randomly split into training (858) and test (215) sets. The classification models built by the ASNN and DLCA MLTs (Table 1) calculated the best performances. For this analysis, E-state, ALOGPS, and CDK2 descriptors were included in the best models for the ASNN method. The results are partially summarized in Table 1. Other statistical parameters and characteristics of individual models are shown in Figure S1 of the Supplementary Materials.

All models had a similar performance by specificity, sensitivity, and BA. The BAs for the training sets were 83-85 % (Table 1). The compounds in the test sets were predicted with similar accuracies (BA = 88-89%). The statistical parameters of training and test sets have large standard mean errors due to small dataset sizes. Despite some variations, both sets' model performances were not significantly different.

**Table 1.** Statistical coefficients calculated for classification models.

N	Method	Sensitivity (%)		Specificity (%)		Balanced accuracy (%)	
		Training	Test	Training	Test	Training	Test
1	DLCA	81	82	89	95	85 ± 1	88 ± 2
2	ASNN	79	83	86	95	83 ± 1	89 ± 2
3	Consensus	80	82	89	95	85 ± 1	88 ± 2

A consensus model was constructed as a simple average of the two individual models. Although its statistical parameters are similar to those of individual models (Table 1), the variance of the consensus model was anticipated to be lower. In addition, consensus model predictions were used to estimate its applicability domain.

A virtual dataset consisting of ten 4-iminohydantoin sulfamides with different substitution patterns (Table S1 in Supplementary materials) was generated based on the recommendation of an experienced synthetic organic chemist. Four compounds predicted as low active as well as one compound predicted outside of the applicability domain, were excluded. The rest five compounds were selected for synthesis and testing (Table S1 in Supplementary materials).

3.2. Chemistry.

For the obtaining of new 4-iminohydantoin sulfamides **1-3, 6, 8** it was used the reaction of 2-amino-3,3-dichloroacrylonitrile (ADAN) **I** [42] with chlorosulfonyl isocyanate [33] followed by (Z)-[5-(dichloromethylene)-2-oxoimidazolidin-4-ylidene]sulfamoyl chloride **II** formation (Scheme 1). The next step is the interaction of sulfonyl chloride **II** with amines in the presence of an excess of amine or triethylamine, leading to sulfonamides **1-3, 6, 8** [33].
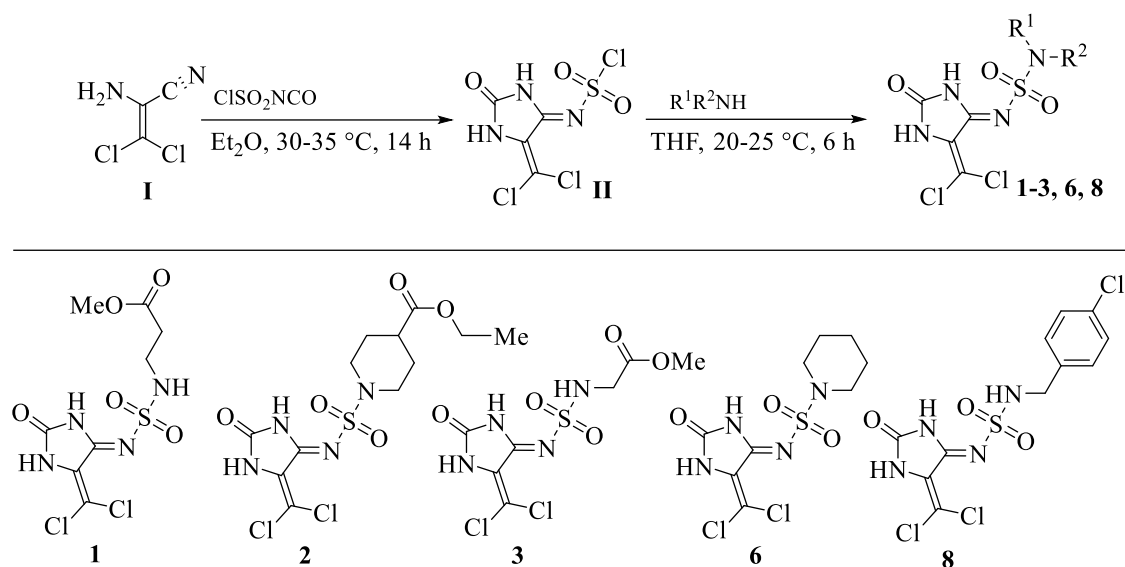
Scheme 1. Synthesis of (Z)-(5-(dichloromethylene)-2-oxoimidazolidin-4-ylidene)sulfamides **1-3, 6, 8**.

The structure of synthesized compounds **1-3, 6,** and **8** were confirmed by the ^{1}H, ^{13}C NMR, and elemental analysis (see Material and Methods).

3.3. Antibacterial testing

In vitro antibacterial activity results of studied 4-iminohydantoin sulfamides with predicted high activity against a panel of selected Gram-negative multidrug-resistant (MDR) *A. baumannii* strains are summarized in Table 2.

Table 2. *In vitro* anti-*A. baumannii* activity of 4-iminohydantoin sulfamides with predicted activity.

Compound	Zone diameter of growth inhibition of MDR *A. baumannii* strains, mm		
	A. baumannii 1355	*A. baumannii* 1536	*A. baumannii* 725
1	18	13	16
2	20	11	12
3	16	11	8
6	22	14	8
8	28	19	18

Table 2 shows the sensitivity of all *A. baumannii* bacteria tested against the 4-iminohydantoin sulfamides. The diameters of inhibition zones of studied derivatives against

MDR *A. baumannii* strains were in the range of 8-28 mm. The most sensitive MDR *A. baumannii* 1355 strain, has demonstrated sensitivity to all compounds in the range from 16 to 28 mm by diameters of growth inhibition. The most active compound **8** seems to be effective against several MDR *A. baumannii* isolates from hospitalized patients.

3.4. Docking procedure.

An *A. baumannii* methionine aminopeptidase (MAP) homology model was created based on the amino acid sequence of *A. baumannii* methionine aminopeptidase (UniProt: A0A059ZMR7) [43] using the SWISS-MODEL homology modeling server. The homology model was built based on template 4a6w.1.A with 1.46 Å resolution, 55.81% sequence identity, and 0.47 sequence similarity characteristics. The created homology model is the most optimal considering the resolution (1.46 Å) and quality characteristics: QMEAN (0.84), GMQE (0.86). The quality of the homology model was also evaluated using the internal resources of the modeling server SWISS-MODEL and SAVESv6.0 Structure Validation Server [44]. The results of the Ramachandran plot showed good quality: 91.7% of amino acid residues were in the most favored regions, 7.8% in additional allowed regions, 0.0% in generously allowed regions, and 0.5% in disallowed regions (Figure 1S). Figure 2S shows the overall quality factor is 94.6939 obtained from the ERRAT2 program [45]. The created homology model was used for docking compound **8** into the active site of *A. baumannii* MAP (Figure 1).
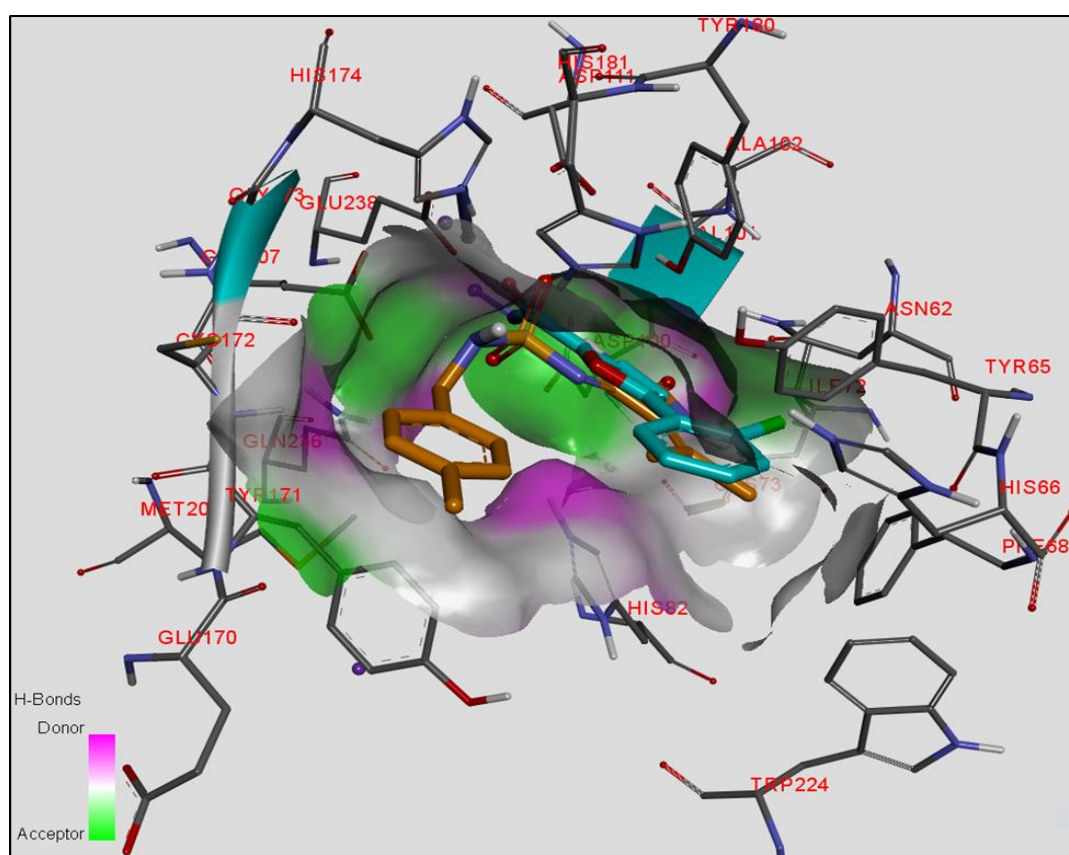

Figure 1. Localization the ligand **8** into the active site of the *A. baumannii* MAP model, blue - inhibitor YE6; orange – compound 8.

The docking results show the formation of the protein-ligand complex with estimated binding energies of −9.3 kcal/mol. It should be noted that the complexation of compound **8** occurs in the active site of *A. baumannii* MAP, similar to inhibitor YE6 co-crystallized with the *E. coli* MAP (PDB ID: 2P99). The obtained high calculated values of the binding energies

of docking and similar docking position compound **8** and inhibitor YE6 confirm the correct docking strategy. The structure and chemical properties of compounds are in good agreement with complexation in the MAP active site in the region with polar amino acid residues. The formation of bonds during the complexation of ligand **8** in the MAP active site is shown in Figure 2.
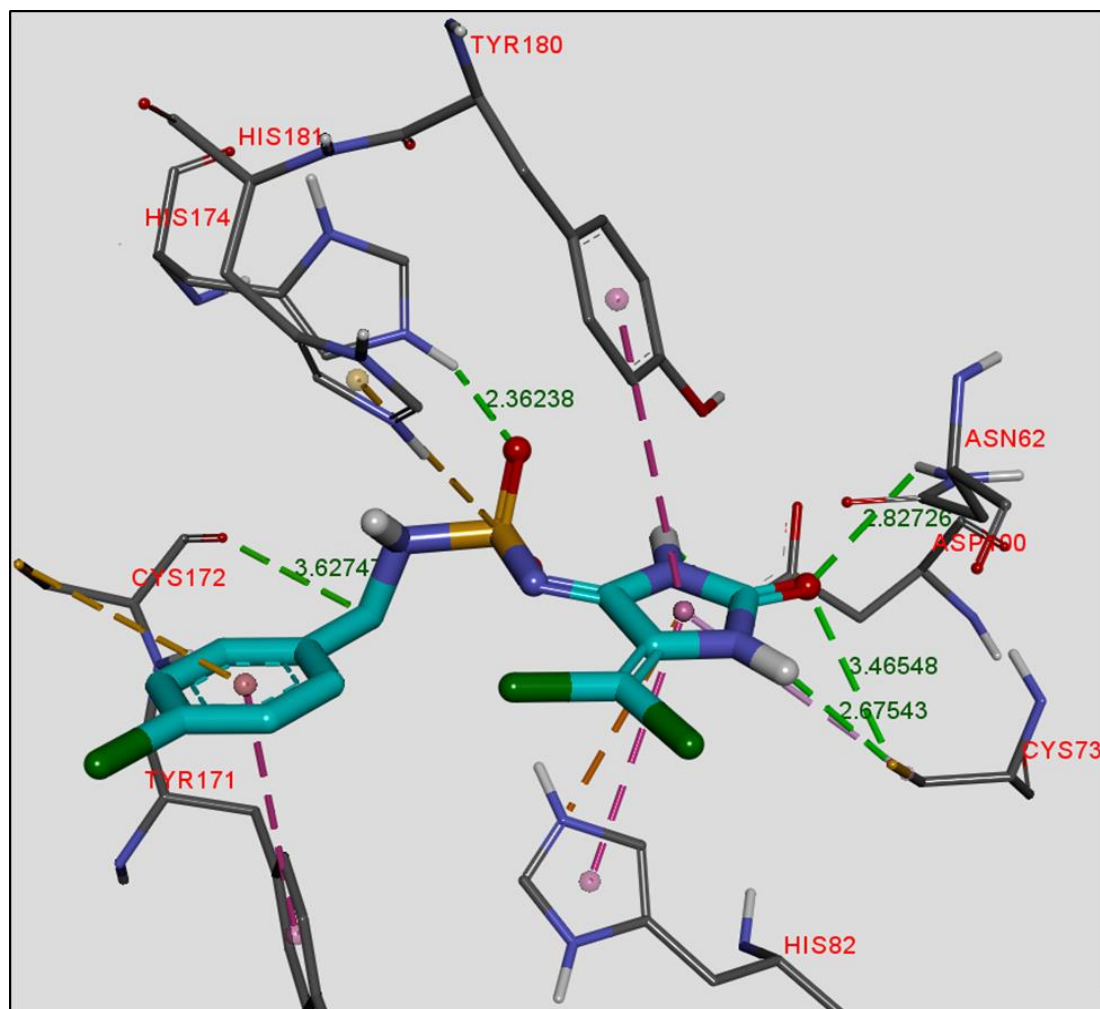

Figure 2. Molecular docking the ligand 8 into the active site of *A. baumannii* MAP model; blue – compound **8**.

The oxoimidazolidine group forms the tree hydrogen bonds (2.67 - 3.46 Å) with amino acids Cys73, Asn62, and Asp100, one electrostatic interaction (4.04 Å) with amino acid His82 and hydrophobic tree interactions (4.75 - 5.54 Å) with amino acids His82, Cys73, and Tyr180. The sulfamide group forms a hydrogen bond (2.36 Å) with His174 and pi-sulfur interaction (4.74 Å) with His181. The aromatic ring forms a hydrogen bond (3.62 Å) with Cys172, hydrophobic interaction (4.79 Å) with amino acid Tyr171, and pi-sulfur interaction (5.38 Å) with Cys172. Thus, the oxoimidazolidine group, the sulfamide group, and the aromatic ring of the ligand **8** participate in the complexation into the active site of the *A. baumannii* MAP model.

4. Conclusions

The current study presents a new anti-*A. baumannii* activity results from synthetic 4-iminohydantoin sulfamides using *in silico* and *in vitro* methods. A number of created predictive QSAR models built using the OCHEM platform with good robustness, stability, and predictive power can be used to search and analyze the new antibacterial agents of appropriate structure

and mechanism of action. It will be helpful for structure optimization to improve the anti-*A. baumannii* activity.

The five 4-iminohydantoin sulfamides identified based on the QSAR modeling had different levels of antibacterial potential against antibiotic-resistant clinical isolates of *A. baumannii*. 4-Iminohydantoin sulfamide **8** showed the highest activity against all studied MDR *A. baumannii* strains with diameters of bacterial growth inhibition in the range from 18 to 28 mm and has substantial potential for therapeutic application as a new drug candidate against MDR bacterial infections.

Molecular docking demonstrated that the high antibacterial activity of all compounds could be associated with the specific binding of the MAP enzyme. Complexation of the ligand **8** in the active center of *A. baumannii* MAP followed the binding energy estimation of − 9.3 kcal/mol. The Cys73, Asn62, Asp100, His174, and Cys172 amino acids play a key role in the ligand-MAP complexes formation.

Funding

Acknowledgments

Conflicts of Interest

The authors declare no conflict of interest.

References

1. Ibrahim, S.; Al-Saryi, N.; Al-Kadmy, I.M.S.; Aziz, S.N. Multidrug-resistant *Acinetobacter baumannii* as an emerging concern in hospitals. *Mol Biol Rep*. **2021**, *48*, 6987-6998, https://doi.org/10.1007/s11033-021-06690-6.

2. Mancuso, G.; Midiri, A.; Gerace, E.; Biondo, C. Bacterial Antibiotic Resistance: The Most Critical Pathogens. *Pathogens* **2021**, *10*, 1310, https://doi.org/10.3390/pathogens10101310.

3. Yasir, M.; Subahi, A.M.; Shukri, H.A.; Bibi, F.; Sohrab, S.S.; Alawi, M.; Sindi, A.A.; Jiman-Fatani, A.A.; Azhar, E.I. Bacterial Community and Genomic Analysis of Carbapenem-Resistant *Acinetobacter baumannii* Isolates from the Environment of a Health Care Facility in the Western Region of Saudi Arabia. *Pharmaceuticals* **2022**, *15*, 611, https://doi.org/10.3390/ph15050611.

4. Sacco, F.; Visca, P.; Runci, F.; Antonelli, G.; Raponi, G. Susceptibility Testing of Colistin for *Acinetobacter baumannii*: How Far Are We from the Truth? *Antibiotics (Basel)* **2021**, *10*, 48, https://doi.org/10.3390/antibiotics10010048.

5. Appaneal, H.J.; Lopes, V.V.; LaPlante, K.L.; Caffrey, A.R. Treatment, Clinical Outcomes, and Predictors of Mortality among a National Cohort of Admitted Patients with *Acinetobacter baumannii* Infection. *Antimicrob Agents Chemother*. **2022**, *66*, e0197521, https://doi.org/10.1128/AAC.01975-21.

6. Karakonstantis, S.; Ioannou, P.; Samonis, G.; Kofteridis, D.P. Systematic Review of Antimicrobial Combination Options for Pandrug-Resistant *Acinetobacter baumannii*. Antibiotics **2021**, *10*, 1344, https://doi.org/10.3390/antibiotics10111344.

7. Lynch III, J.P.; Clark, N.M.; Zhanel, G.G. Infections Due to Acinetobacter baumannii–calcoaceticus Complex: Escalation of Antimicrobial Resistance and Evolving Treatment Options. *Semin Respir Crit Care Med* **2022**, *43*, 097-124, https://doi.org/10.1055/s-0041-1741019.

8. Alrahmany, D.; Omar, A.F.; Alreesi, A.; Harb, G.; Ghazi, I.M. *Acinetobacter baumannii* Infection-Related Mortality in Hospitalized Patients: Risk Factors and Potential Targets for Clinical and Antimicrobial Stewardship Interventions. *Antibiotics* **2022**, *11*, 1086, https://doi.org/10.3390/antibiotics11081086.

9. Zeidler, S.; Müller, V. The role of compatible solutes in desiccation resistance of *Acinetobacter baumannii*. *Microbiologyopen* **2019**, *8*, e00740, https://doi.org/10.1002/mbo3.740.

10. Gedefie, A.; Demsis, W.; Ashagrie, M.; Kassa, Y.; Tesfaye, M.; Tilahun, M.; Bisetegn, H.; Sahle, Z. *Acinetobacter baumannii* Biofilm Formation and Its Role in Disease Pathogenesis: A Review. *Infect Drug Resist*. **2021**, *14*, 3711-3719, https://doi.org/10.2147/IDR.S332051.

11. Higgins, P.G.; Hagen, R.M.; Podbielski, A.; Frickmann, H.; Warnke, P. Molecular Epidemiology of Carbapenem-Resistant Acinetobacter baumannii Isolated from War-Injured Patients from the Eastern Ukraine. *Antibiotics* **2020**, *9*, 579, https://doi.org/10.3390/antibiotics9090579.

12. Ruan, B.F.; Guo, Q.L.; Li, Q.S.; Li, L.Z.; Deora, G.S.; Zhou, B.G. A Review of the Biological Activities of Heterocyclic Compounds Comprising Oxadiazole Moieties. *Curr Top Med Chem*. **2022**, *22*, 578-599, https://doi.org/10.2174/1568026622666220202123651.

13. Li, M.; Chen, X.; Deng, Y.; Lu, J. Recent advances of N-heterocyclic carbenes in the applications of constructing carbo- and heterocyclic frameworks with potential biological activity. *RSC Adv*. **2021**, *11*, 38060-38078, https://doi.org/10.1039/D1RA06155K.

14. Salehian, F.; Nadri, H.; Jalili-Baleh, L.; Youseftabar-Miri, L.; Abbas Bukhari, S.N.; Foroumadi, A.; Tüylü Küçükkilinç, T.; Sharifzadeh, M.; Khoobi, M. A review: Biologically active 3,4-heterocycle-fused coumarins. *Eur J Med Chem*. **2021**, *212*, 113034, https://doi.org/10.1016/j.ejmech.2020.113034.

15. Ebenezer, O.; Jordaan, M.A.; Carena, G.; Bono, T.; Shapi, M.; Tuszynski, J.A. An Overview of the Biological Evaluation of Selected Nitrogen-Containing Heterocycle Medicinal Chemistry Compounds. *Int. J. Mol. Sci*. **2022**, *23*, 8117, https://doi.org/10.3390/ijms23158117.

16. Janovec, L.; Kožurková, M.; Sabolová, D.; Ungvarský, J.; Paulíková, H.; Plšíková, J.; Vantová, Z.; Imrich, J. Cytotoxic 3,6-bis((imidazolidinone)imino)acridines: synthesis, DNA binding and molecular modeling. *Bioorg Med Chem*. **2011**, *19*, 1790-801. https://doi.org/10.1016/j.bmc.2011.01.012.

17. Wei, L.; Gan, X.; Zhong, J.; Alliston, K.R.; Groutas, W.C. Noncovalent inhibitors of human leukocyte elastase based on the 4-imidazolidinone scaffold. *Bioorg Med Chem*. **2003**, *11*, 5149-53, https://doi.org/10.1016/j.bmc.2003.08.030.

18. Ali, A.; Reddy, G.S.; Cao, H.; Anjum, S.G.; Nalam, M.N.; Schiffer, C.A.; Rana, T.M. Discovery of HIV-1 protease inhibitors with picomolar affinities incorporating N-aryl-oxazolidinone-5-carboxamides as novel P2 ligands. *J Med Chem*. **2006**, *49*, 7342-56, https://doi.org/10.1021/jm060666p.

19. Weng, Z.; Shao, X.; Graf, D.; Wang, C.; Klein, C.D.; Wang, J.; Zhou, G.C. Identification of fused bicyclic derivatives of pyrrolidine and imidazolidinone as dengue virus-2 NS2B-NS3 protease inhibitors. *Eur J Med Chem*. **2017**, *125*, 751-759, https://doi.org/10.1016/j.ejmech.2016.09.063.

20. González-Bacerio, J.; Varela, A.C.; Aguado, M.E.; Izquierdo, M.; Méndez, Y.; Del Rivero, M.A.; Rivera, D.G. Bacterial Metalo-Aminopeptidases as Targets in Human Infectious Diseases. *Curr Drug Targets* **2022**, *23*, 1155-1190, https://doi.org/10.2174/1389450123666220316085859.

21. Omar, M.N.; Raja Abd Rahman, R.N.Z.; Muhd Noor, N.D.; Latip, W.; Knight, V.F.; Ali, M.S.M. Structure-Function and Industrial Relevance of Bacterial Aminopeptidase P. *Catalysts* **2021**, *11*, 1157, https://doi.org/10.3390/catal11101157.

22. ChEMBL. https://www.ebi.ac.uk/chembl/.

23. Sushko, I.; Novotarskyi, S.; Körner, R.; Pandey, A.K.; Rupp, M.; Teetz, W.; Brandmaier, S.; Abdelaziz, A.; Prokopenko, V.V.; Tanchuk, V.Y.; Todeschini, R.; Varnek, A.; Marcou, G.; Ertl, P.; Potemkin, V.; Grishina, M.; Gasteiger, J.; Schwab, C.; Baskin, I.I.; Palyulin, V.A.; Radchenko, E.V.; Welsh, W.J.; Kholodovych, V.; Chekmarev, D.; Cherkasov, A.; Aires-de-Sousa, J.; Zhang, Q.Y.; Bender, A.; Nigsch, F.; Patiny, L.; Williams, A.; Tkachenko, V.; Tetko, I.V. Online chemical modeling environment (OCHEM): web platform for data storage, model development and publishing of chemical information. *J. Comput. Aided. Mol. Des*. **2011**, *25*, 533-554, https://doi.org/10.1007/s10822-011-9440-2.

24. Tetko, I.V. Associative neural network. *Methods Mol Biol*. **2008**, *458*, 185-202, https://doi.org/10.1007/978-1-60327-101-1_10.

25. Zakharov, A.V.; Zhao, T.; Nguyen, D.T.; Peryea, T.; Sheils, T.; Yasgar, A.; Huang, R.; Southall, N.; Simeonov, A. Novel consensus architecture to improve performance of large-scale multitask deep learning QSAR Models. *J Chem Inf Model*. **2019**, *59*, 4613-4624, https://doi.org/10.1021/acs.jcim.9b00526.

26. Hall, L.H.; Kier, L.B. Electrotopological State Indexes for Atom Types—A Novel Combination of Electronic, Topological, and Valence State Information. *J Chem Inf Comput Sci*. **1995**, *35*, 1039–1045, https://doi.org/10.1021/ci00028a014.

27. Tetko, I.V.; Tanchuk, V.Y. Application of associative neural networks for prediction of lipophilicity in ALOGPS 2.1 program. *J Chem Inf Comput Sci*. **2002**, *42*, 1136–1145, https://doi.org/10.1021/ci025515j.

28. Willighagen, E.L.; Mayfield, J.W.; Alvarsson, J.; Berg, A.; Carlsson, L.; Jeliazkova, N.; Kuhn, S.; Pluskal, T.; Rojas-Chertó, M.; Spjuth, O.; Torrance, G.; Evelo, C.T.; Guha, R.; Steinbeck, C. The Chemistry Development Kit (CDK) v2.0: atom typing, depiction, molecular formulas, and substructure searching. *J Cheminform*. **2017**, *9*, 33, https://doi.org/10.1186/s13321-017-0220-4.

29. Whitley, D.C.; Ford, M.G.; Livingstone, D.J. Unsupervised forward selection: A method for eliminating redundant variables. *J. Chem. Inf. Comput. Sci*. **2000**, *40*, 1160–1168, https://doi.org/10.1021/ci000384c.

30. Tetko, I.V.; Sushko, I.; Pandey, A.K.; Zhu, H.; Tropsha, A.; Papa, E.; Oberg, T.; Todeschini, R.; Fourches, D.; Varnek, A. Critical assessment of QSAR models of environmental toxicity against Tetrahymena pyriformis: focusing on applicability domain and overfitting by variable selection. *J Chem Inf Model*. **2008**, *48*, 1733-46, https://doi.org/10.1021/ci800151m.

31. Sushko, I.; Novotarskyi, S.; Körner, R.; Pandey, A.K.; Kovalishyn, V.V.; Prokopenko, V.V.; Tetko, I.V. Applicability domain for in silico models to achieve accuracy of experimental measurements. *J Chemom*, **2010**, *24*, 202–208, https://doi.org/10.1002/cem.1296.

32. OCHEM docs. https://docs.ochem.eu/display/MAN.html.

33. Shablykin, O.V.; Kornii, Yu.Eu.; Dyakonenko, V.V.; Shablykina, O.V.; Brovarets, V.S. Synthesis and anticancer activity of new substituted imidazolidinone sulfonamides. *Curr. Chem. Lett*., **2019**, *8*, 199-210, https://doi.org/10.5267/j.ccl.2019.5.003.

34. Bauer, A.W.; Kirby,W.M.; Sherris, J.C.; Turck, M. Antibiotic Susceptibility Testing by a Standardized Single Disk Method. *Am. J.Clin. Pathol*. **1966**, *45*, 493–496, https://pubmed.ncbi.nlm.nih.gov/5325707/.

35. Waterhouse, A.; Bertoni, M.; Bienert, S.; Studer, G.; Tauriello, G.; Gumienny, R.; Heer, F.T.; de Beer, T.A.P.; Rempfer, C.; Bordoli, L.; Lepore, R.; Schwede, T. SWISS-MODEL: homology modelling of protein structures and complexes. *Nucleic Acids Research* **2018**, *46*, W296–W303, https://doi.org/10.1093/nar/gky427.

36. Sanner, MF. Python: a programming language for software integration and development. *J Mol Graph Model*. **1999**, *17*, 57-61, https://pubmed.ncbi.nlm.nih.gov/10660911/.

37. MarvinSketch 5.3.735, 2017. http://www.chemaxon.com.

38. Hanwell, M.D.; Curtis, D.E.; Lonie, D.C.; Vandermeersch, T.; Zurek, E.; Hutchison, G.R. Avogadro: an advanced semantic chemical editor, visualization, and analysis platform. *J Cheminform*. **2012**, *4*, 17, https://doi.org/10.1186/1758-2946-4-17.

39. Trott, O.; Olson, A.J. AutoDock Vina: improving the speed and accuracy of docking with a new scoring function, efficient optimization, and multithreading. *J Comput Chem*. **2010**, *31*, 455-61, https://doi.org/10.1002/jcc.21334.

40. https://www.rcsb.org/structure/2P98.

41. Discovery Studio Visualizer, v4.0.100.13345. Available from: https://discover.3ds.com/ (accessed on October 12, 2022).

42. Matsumura, K.; Saraie, T.; Hashimoto, N. Studies of Nitriles. VII. Synthesis and Properties of 2-Amino-3,3-dichloroacrylonitrile (ADAN). *Chem. Pharm. Bull*. **1976**, *24*, 912-923, https://doi.org/10.1248/cpb.24.912.

43. The UniProt Consortium, UniProt: the universal protein knowledgebase, *Nucleic Acids Research*, **2018**, *46*, 2699, https://doi.org/10.1093/nar/gky092.

44. https://saves.mbi.ucla.edu/.

45. Colovos, C.; Yeates, T.O. Verification of protein structures: patterns of nonbonded atomic interactions. *Protein Sci*. **1993**, *2*, 1511-9, https://doi.org/10.1002/pro.5560020916.

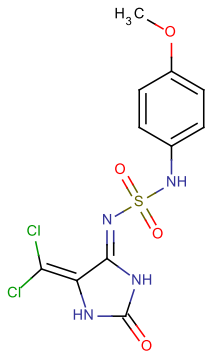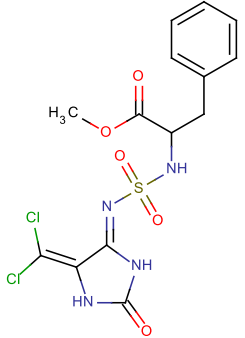**Supplementary Material**
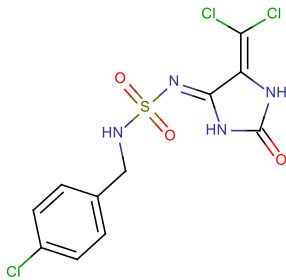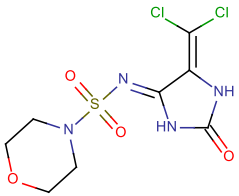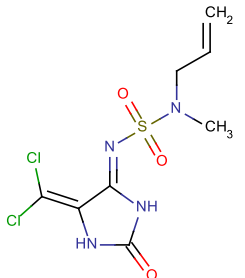
Classification machine learning models
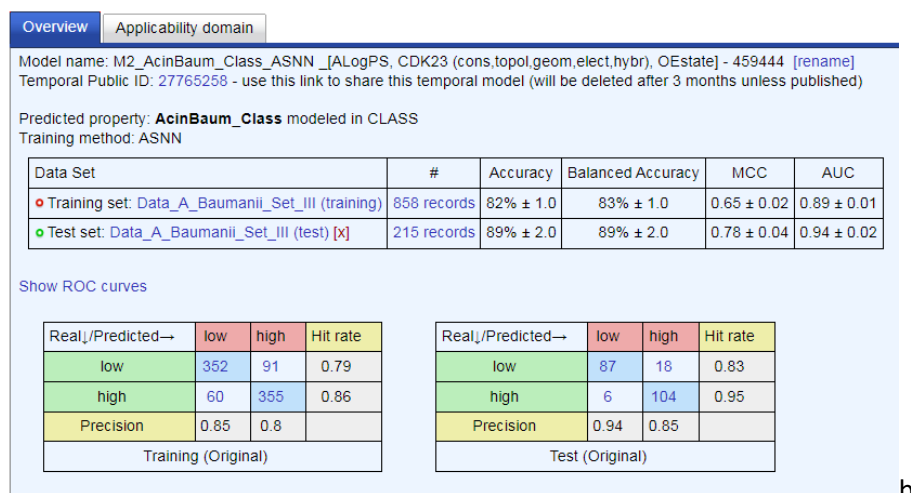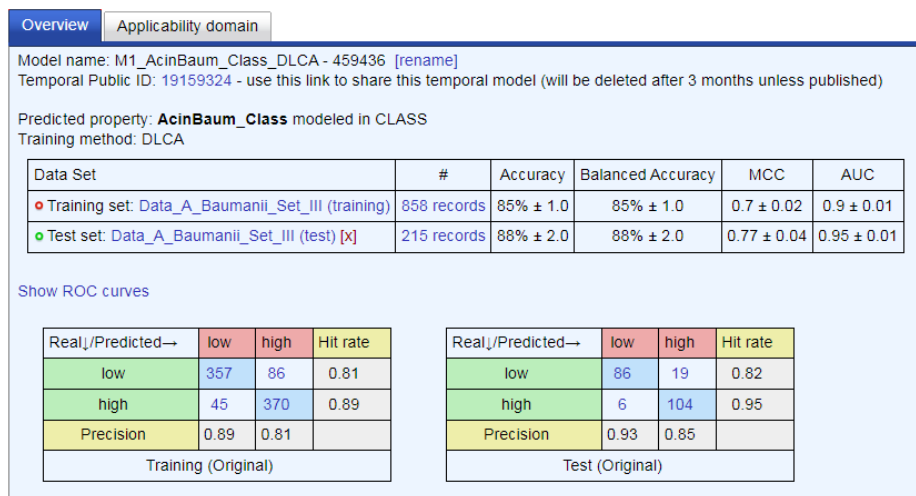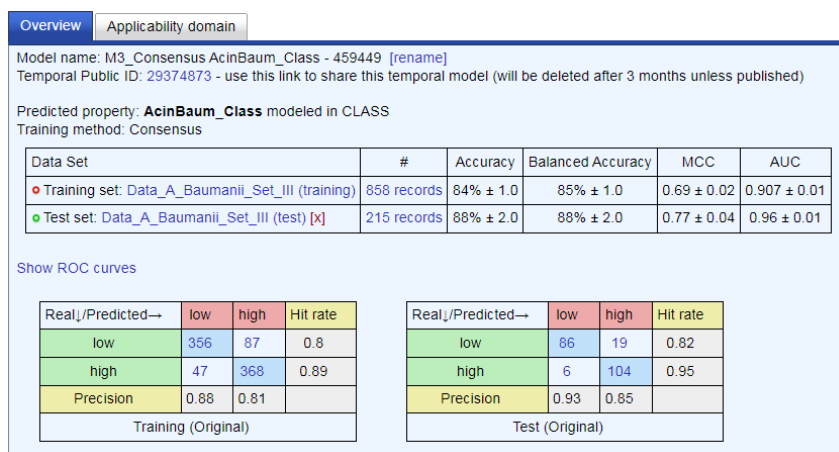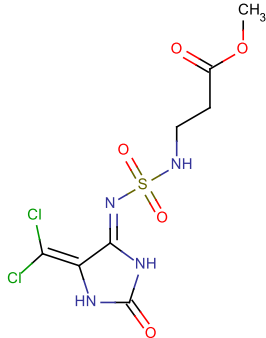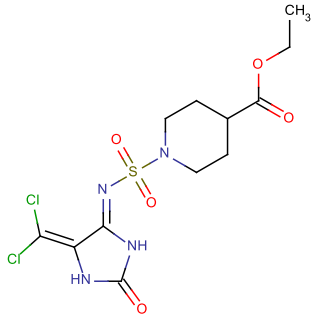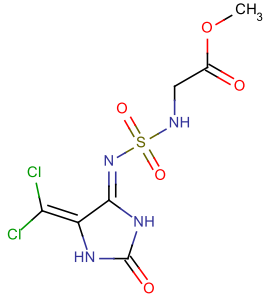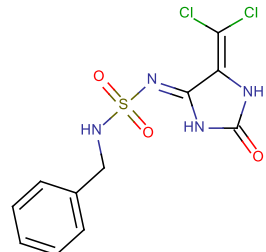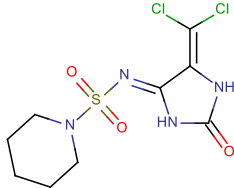
Figure 1S. Classification machine learning models built by the OCHEM server for data; a-b) Performance statistics of binary classifiers; c) Consensus model calculated on the basis of previous 2 models.

Evaluation antibacterial activity of new compounds

Table S1. Antibacterial activity calculated by using the consensus classification models for virtual set of imidazole derivatives.

Compound No	Chemical Structure	Pred. activity	CONSENSUS-STD	Estimated accuracy	AD
1ᵃ		high	0.14	0.79	TRUE
2ᵃ		high	0.06	0.87	TRUE
3ᵃ		high	0.06	0.9	TRUE
4		low	0.15	0.79	TRUE
5		low	0.12	0.86	TRUE

Compound No	Chemical Structure	Pred. activity	CONSENSUS-STD	Estimated accuracy	AD
6ª		high	0.18	0.74	TRUE
7		low	0.01	0.88	TRUE
8ª		high	0.03	0.91	TRUE
9		low	0.06	0.87	TRUE
10		high	0.33	0.66	FALSE

ªFinal set of compounds are represented in bold. CONSENSUS-STD – the standard deviation of the predictions, obtained from an ensemble of models.